JOURNAL OF THERMOPHYSICS AND HEAT TRANSFER
Vol. 25, No. 3, July–September 2011

Electronic Excitation of Atoms and Molecules for the FIRE II Flight Experiment

M. Panesi*
von Kármán Institute for Fluid Dynamics, 1640 Rhode-Saint-Genèse, Belgium
T. E. Magin†
Stanford University, Stanford, California 94305
A. Bourdon‡
École Centrale Paris, 92290 Chatenay-Malabry, France
A. Bultel§
Université de Rouen, 76800 Saint-Etienne du Rouvray, France
and
O. Chazot¶
von Kármán Institute for Fluid Dynamics, 1640 Rhode-Saint-Genèse, Belgium

DOI: 10.2514/1.50033

An accurate investigation of the behavior of electronically excited states of atoms and molecules in the postshock relaxation zone of a trajectory point of the Flight Investigation of Reentry Environment 2 (FIRE II) flight experiment is carried out by means of a one-dimensional flow solver coupled to a collisional-radiative model. The model accounts for thermal nonequilibrium between the translational energy mode of the gas and the vibrational energy mode of individual molecules. Furthermore, electronic states of atoms and molecules are treated as separate species, allowing for non-Boltzmann distributions of their populations. In the rapidly ionizing regime behind a strong shock wave, the high-lying bound electronic states of atoms are depleted. This leads to the electronic energy level populations of atoms departing from the Boltzmann distributions. For molecular species, departures from Boltzmann equilibrium are limited to a narrow zone close to the shock front. A comparison with the recent model derived by Park (Park, C., "Parameters for Electronic Excitation of Diatomic Molecules 1. Electron-Impact Processes," 46th AIAA Aerospace Sciences Meeting and Exhibit, Reno, NV, AIAA Paper 2008-1206, 2008.) shows adequate agreement for predictions involving molecules. However, the predictions of the electronic level populations of atoms differ significantly. Based on the detailed collisional-radiative model developed, a reduced kinetic mechanism has been designed for implementation into two-dimensional or three-dimensional flow codes.

I. Introduction

IN RECENT years, space agencies such as NASA and ESA have shown a renewed interest in the manned space exploration, aiming at transporting humans to the moon, and eventually to Mars. One risky phase, common to all manned missions, is the reentry into the Earth's atmosphere. The space vehicles, interacting with the atmosphere at near-orbital or superorbital speeds, are subjected to a strong deceleration: the freestream kinetic energy is converted into translational energy of the fluid particles through a bow shock. This energy transfer is associated with numerous physicochemical processes that occur in the shock layer, from excitation of the internal energy modes of the atoms and molecules to different chemical reactions, such as molecular dissociation and atomic and molecular ionization. These collisional and radiative phenomena are tightly coupled to each other and often happen far from local thermodynamic equilibrium, requiring an accurate calculation of the populations of the internal energy levels for both atoms and molecules. In the literature, a considerable effort has been devoted to understanding the chemistry of shock-heated air [1–7] for an improved accuracy of the heat flux prediction and a better interpretation of experimental measurements.

In [1], we have reviewed the different kinds of collisional-radiative (CR) models available in the literature to study nonequilibrium air chemistry, and we have developed a simplified hybrid model for air by combining an electronic CR model for the electronic energy levels of atoms with a multitemperature model, which describes the thermochemical nonequilibrium effects for all the other energy modes of the gas species. This so-called atomic ABBA model has been coupled with a one-dimensional (1-D) flow solver and applied to simulations of the Flight Investigation of Reentry Environment 2 (FIRE II) experiment [8], a high-speed reentry flight experiment carried out in 60 s to address uncertainties in the aerothermodynamic models used in the development of the Apollo thermal protection system. We have previously studied three points of the flight trajectory: 1634, 1636, and 1643 s (elapsed time from the launch). The first two points belong to the early part of the trajectory, where the flow exhibits strong nonequilibrium effects, whereas for the last point under consideration, the gas is close to equilibrium conditions. To quantify the extent of these nonequilibrium effects, the results obtained by means of the atomic ABBA model have been compared with those based on Boltzmann distributions. We have found a

Presented as Paper 2008-1205 at the 46th AIAA Aerospace Sciences Meeting and Exhibit, Reno, NV, 7–10 January 2008; received 24 March 2010; revision received 13 December 2010; accepted for publication 7 January 2011.

*Aeronautics and Aerospace Department, chaussée de Waterloo 72; currently Postdoctoral Fellow, Institute for Computational Engineering and Sciences, University of Texas at Austin,201 East 24th Street, Texas 78712; mpanesi@ices.utexas.edu.

†Center for Turbulence Research, 488 Escondido Mall; currently Assistant Professor, Aeronautics and Aerospace Department, von Kármán Institute for Fluid Dynamics, chaussée de Waterloo 72, 1640 Rhode-Saint-Genèse, Belgium; magin@vki.ac.be.

‡CNRS Research Fellow, EM2C Laboratory, CNRS UPR 288, Grande voie des vignes; anne.bourdon@em2c.ecp.fr.

§Assistant Professor, CORIA, CNRS UMR 6614, Site Universitaire du Madrillet, BP 12; arnaud.bultel@coria.fr.

¶Associate Professor, Aeronautics and Aerospace Department, chaussée de Waterloo 72; chazot@vki.ac.be.

departure of the electronic energy level populations of atoms from Boltzmann distributions due to depletion of the high-lying bound electronic states in the rapidly ionizing regime behind the strong shock wave. For the earliest trajectory point considered (in [1]), we have also shown that the quasi-steady-state (QSS) assumption is only valid for the high-lying excited electronic states and cannot be used to model the metastable states of atoms.

In the present work, we propose to more accurately model the nonequilibrium effects in the postshock region by abandoning the Maxwell–Boltzmann distribution hypothesis on the electronic energy level populations for the molecules and molecular ions. The rovibrational energy level populations of the ground and excited electronic states of molecules and molecular ions are still assumed to follow Maxwell–Boltzmann distributions at distinct rotational (translational) and vibrational temperatures. The CR model developed (more complete than the atomic ABBA model) is referred to as the full ABBA model. The latter model is then coupled with a 1-D flow solver and applied to simulate the trajectory point at 1634 s for the reentry trajectory of the FIRE II flight experiment, seeing that the most significant nonequilibrium effects on the electronic energy level populations of atoms have already been observed for this point in [1]. The sensitivity of the reaction rate coefficients on the electronic energy population is also assessed by comparing our predictions with the results obtained by means of the electronic CR model for air plasmas, recently developed by Park [9,10] and Hyun et al. [11] and included in the SPRADIAN code.

Electronic CR models prove to be powerful tools for a thorough investigation of nonequilibrium effects in zero-dimensional and 1-D simulations. However, owing to the large number of species and reactions involved, it remains unrealistic to directly couple such detailed models with two-dimensional (2-D) and three-dimensional (3-D) flow solvers. The loosely coupled QSS approach, extensively discussed in [12,13], allows us to take into account a large number of species, but it requires ad hoc assumptions for the flowfield calculations; its general use cannot be recommended. A deeper discussion of the QSS approach is found in [14–17]. Thus, in order to apply the model with 2-D and 3-D flow solvers for CFD applications, the number of pseudospecies included in the CR model has to be reduced [18]. The idea of grouping atomic levels was already presented in [19], and in some references therein. However, the simplified model presented in [19] aims at calculating partition functions and thermodynamic properties of atomic species. The correct modeling of the thermodynamic properties of a gas is indeed a fundamental prerequisite of a reduced model; however, it does not guarantee the accurate representation of the chemical kinetics of the studied gas mixture.

In this work, using as reference the full ABBA model, we propose to derive a reduced CR model based on a combination of real and lumped electronic states for atoms. Many studies have been done on reduced kinetic mechanisms with grouped levels. However, usually, the validity of the way the levels have been grouped is hardly discussed. In our work, we propose to assess the quality of the results delivered by the reduced model by performing direct comparisons of the results from this model and results obtained from the full ABBA model.

The full ABBA model is presented in Sec. II. Section III is devoted to simulation of the shock-tube condition representative of an early trajectory point for FIRE II. The results are compared with the ones obtained by means of the atomic ABBA model given in [1], the recent model proposed by Park [9,10] and Hyun et al. [11], and the proposed reduced kinetic mechanism.

II. Physicochemical Modeling

The air mixture used in this work comprises 116 species, including the electronic energy levels of the atoms and molecules as additional pseudospecies, for which the composition is governed by a finite rate chemistry mechanism allowing for nonequilibrium populations to be modeled. The vibrational energy level populations of the N_2, O_2, and NO molecules are assumed to follow Boltzmann distributions at the vibrational temperatures T_{vN_2}, T_{vO_2}, and T_{vNO}, respectively; the vibrational populations for the other molecules are associated with the vibration of the N_2 molecule. The rotational energy level populations are assumed to follow Boltzmann distributions at the translational temperature T of the gas. Certainly, the use of identical vibrational temperatures for different electronic states of the diatomic molecules is a limitation of the current CR model. In the future, we plan to work on the more accurate modeling of the vibrational excitation of the different molecules in their different electronic states. However, it is important to note that, in general, the accurate modeling of the rovibrational excitation of the electronic states of the molecular species is a cumbersome task, requiring the knowledge of a large number of relaxation parameters, which are often unavailable. Supposedly, in fact, the upper vibrational levels of the electronically excited states quickly dissociate (or recombine), due to the crossing of their potential with repulsive states, and their population may strongly deviate from a Maxwell–Boltzmann distribution, thus requiring the use of a state-to-state model, as discussed in [20]. In this work, the CR model yields the electronic state populations of all the atoms and molecules, except for the atomic ions. Thus, their electronic temperature does not need to be specified, except for N^+ and O^+, for which the populations are assumed to follow Boltzmann distributions. In general, the excitation of the internal structure of chemical species in the mixture is mainly due to the light particles (electrons); therefore, the free-electron temperature should be the one used to describe the population of the atomic states of the atomic ions. However, as shown in [1], thermal nonequilibrium between the free-electron energy/Boltzmann electronic energy and the vibrational energy of N_2 is restricted to a narrow zone after the shock. In this case, the thermal nonequilibrium effect has a negligible influence on the evolution of the postshock temperatures and the atomic electronic energy populations. Therefore, as already done in [1], we have assumed that the electronic energy populations of N^+ and O^+ ions follow Boltzmann distributions at the vibrational temperature T_{vN_2}. Also, the degree of dissociation of the gas may affect the validity of this assumption, since dissociation processes consume the nitrogen molecules. In the case under investigation, however, the concentration of nitrogen molecules is comparable to the one of the atomic species in the postshock region where the temperature of the free electron departs from T_{vN_2}. A possible alternative would be to consider the use of the electronic temperature of atomic nitrogen whenever it is possible to define such a temperature. However, the analysis presented clearly shows how the population of the atomic nitrogen departs from the Maxwell–Boltzmann distribution. For this reason, the definition of an electronic temperature becomes, at best, unclear. In the near future, we plan to adopt a state-to-state approach for these chemical components. Deviation of the electron energy distribution function from equilibrium, not considered here, is discussed in [21], where the authors present a CR model for hydrogen atoms coupled to the Boltzmann equation for free-electron kinetics. The study of the influence of a non-Maxwellian electron energy distribution for air and flow conditions of the FIRE II experiment will be presented in a dedicated paper.

A. Air Mixture

In this study, air is considered as a mixture of nitrogen and oxygen and their products, composed of neutral species of N_2(1–4), O_2(1–5), NO(1–5), N(1–46), and O(1–40); and charged species of N_2^+(1–4), O_2^+(1–4), NO^+(1–5), N^+, O^+, and e^-. Ar is neglected, as well as negative ions. Forty-six levels for N atoms [22] and 40 levels

Table 1 Molecules and molecular ions considered in the full ABBA CR model

Type	Species	State
Molecules	N_2 (1–4)	$X^1\Sigma_g^+$, $A^3\Sigma_u^+$, $B^3\Pi_g$, $C^3\Pi_u$
	O_2 (1–5)	$X^3\Sigma_g^-$, $a^1\Delta_g$, $b^1\Sigma_g^+$, $A^3\Sigma_u^+$, $B^3\Sigma_u^-$
	NO (1–5)	$X^2\Pi$, $A^2\Sigma^+$, $B^2\Pi$, $C^2\Pi$, $B'^3\Delta$
Molecular ions	N_2^+ (1–4)	$X^2\Sigma_g^+$, $A^2\Pi_u$, $B^2\Sigma_u^+$, $C^2\Sigma_u^+$
	O_2^+ (1–4)	$X^2\Pi_g$, $a^4\Pi_u$, $A^2\Pi_u$, $b^4\Sigma_g^-$
	NO^+ (1–5)	$X^1\Sigma^+$, $a^3\Sigma^+$, $b^3\Pi$, $b'^3\Sigma^-$, $A^1\Pi$

for O atoms [23] are taken into account, and a total number of 27 levels for the diatomic species, molecules, and molecular ions [2]. Their electronic states are reviewed in Table 1.

B. Collisional-Radiative Model

1. Atomic Elementary Processes

The inelastic collisions between the mixture species lead to chemical changes. The N and O atoms are efficiently excited and ionized by electron impact reactions; due to their weak mass, free electrons very easily change occupation for the attached electrons of atoms. Several models exist for the related cross sections and rate coefficients. For excitation and ionization of the first three electronic states of N and O, we have used the rate coefficients reported by Bultel et al. [2]. The cross sections proposed by Drawin [24,25] are adopted here for excitation and ionization of the higher states. We have expressed the rate coefficients under an analytical form derived from integration of these cross sections over a Boltzmann distribution at the electron temperature [1].

2. Molecular Elementary Processes

The kinetic mechanism comprises different types of forward and backward reactions: excitation/deexcitation by heavy-particle and electron impacts; ionization/recombination by heavy-particle and electron impact; dissociation of N_2, O_2, and NO/recombination of N and O, by atomic or molecular impact; dissociation of N_2/recombination of N by electron impact; associative ionization/dissociative recombination; radical reactions (including Zel'dovich reactions); and charge exchange reactions.

For atoms, the cross sections for electron-induced processes depend on the threshold energy (given by the energy difference between the two electronic states) and the kinetic energy of the impinging free electron [1]. Although these cross sections may depend on the possibility of an optical transition among the two excited states, the threshold is well determined and the reaction rates can easily be obtained, provided that the electron energy distribution is known (it is assumed to be Maxwellian in this work). Similar conclusions hold for excitation/ionization processes among the rovibronic states of the molecular species, i.e., for transitions from the rovibronic state (e_1, v_1, and J_1) to the rovibronic state (e_2, v_2, and J_2). For an electronic CR model, we need to define rate coefficients that are applicable to transitions from molecular electronic level 1 to level 2; these levels are characterized by both their own electronic energy and the averaged rovibrational energy. In this case, the threshold energy is not precisely known: it is a function of the rovibrational excitation of the molecule in the lower state, thus depending on the rotational and vibrational temperatures [26]. Consequently, the resulting rate coefficients also depend on the rotational and vibrational temperatures.

In the present work, we propose to use the rate coefficients for excitation, ionization, and dissociation of molecular species by electron impact, recently calculated by Teulet et al. [27] by estimating the inelastic rate constants using the method of weighted total cross section developed by Bacri and Medani in [26,28,29]. The modifications suggested by Sarrette et al. [30] are introduced to account for predissociation of some electronic states of O_2 and NO in the calculation of the dissociation rate coefficients.

The cross section for excitation of molecules involved in molecular or atomic impact behaves approximately, as explained by Lotz [31]. Therefore, this model has been adopted, except when experimental data exist. We have then used the rate coefficients compiled by Capitelli et al. [32] and Kossyi et al. [33].

Dissociation processes, as well as their coupling with vibration, are of key importance for hypersonic reentry applications, as they significantly affect aerodynamics, the radiative and convective heat fluxes, and the spectral signatures of vehicles flying at suborbital to superorbital velocities in rarefied atmospheres. To determine the population of the internal energy states, it would be more accurate to consider the vibronic states as pseudospecies, then treat inelastic collisions as chemical reactions, and finally compute average quantities for the vibrational–translational, vibrational–vibrational, and vibrational–vibrational–translational processes. This type of model requires a very large number of data in terms of transition rate coefficients. Theoretical calculations have become possible only recently [34–36], but an exhaustive database for air is still lacking.

In this work, we use three models to describe the influence of the vibration on the dissociation of the molecular species and, at the same time, to account for the influence of the chemistry on the vibrational energy:

1) The $T - T_v$ Park model [12] is the most widely spread and used model in the aerospace community, mainly due to its simplicity. The geometrical average temperature $\sqrt{TT_v}$ is used in the Arrhenius law for the rate coefficients. This model is purely heuristic and based on the analysis of experimental data coming from the study of the postshock radiative signature in shock-tube facilities. For this model, we do not use any preferential dissociation model.

2) The Macheret–Fridman model [37] is based on the corrected forced harmonic oscillator (FHO) approach. The FHO model was successfully applied and culminated in an analytical (or semi-analytical) theory with no adjustable parameters, which also consistently accounts for three-dimensionality of collisions and for molecular rotations [38–40]. Such a model with no adjustable parameters has produced thermal equilibrium dissociation rates in excellent agreement with experimental data [40].

3) The Treanor–Marrone model [41] is based on simple physical concepts first introduced by Hammerling et al. [42]. The innovation of the model lies in the introduction of an ad hoc parameter U to change the value of the probability of dissociation among the different energy levels. This results in an increasing dissociation probability with the increasing vibrational level number. Decreasing the semiempirical parameter U induces a relatively stronger increase in the dissociation probabilities of higher levels.

For direct dissociation by molecular impact, the rate coefficients of Park et al. [43] are used. These rates are extrapolated to nonequilibrium conditions using the three models previously discussed. It is important to note that recent quasi-classical trajectory (QCT) calculations for dissociation by atom impact [34,35] agree well with the dissociation coefficients of Park et al. The reverse rates are computed at the gas temperature T based on the equilibrium constant. The rates for the reactions of dissociation of nitrogen and oxygen by electron impact are taken from [44,45], respectively. These dissociation rates and the rates for the reverse processes are computed at the electron temperature.

The dissociative recombination of molecular ions is known to play an important role in the case of recombining plasmas [46,47]. The inverse process, associative ionization, allows for formation of the first electrons in many cases, such as in shock tubes and reentry problems [48]. Consequently, it allows for many ionizing situations to be explained. In our case, since N_2^+, O_2^+, and NO^+ are present in the plasma described here, dissociative recombination has to be considered. Further details are given in [2]. Zel'dovitch reactions are known to greatly influence the distribution of nitrogen and oxygen between atomic and molecular systems and contribute to the destruction of O_2 and N_2 and the formation of NO. We have used the rate coefficients obtained by Bose and Candler [49,50], using a QCT method performed starting from ab initio calculations of the potential energy surface.

3. Radiative Processes

For entry speeds around 10 km/s, relevant for lunar return studies, the main contributors to the radiative heat loads are the line and continuum radiation (i.e., radiative recombination) generated by the N and O atoms [4,51]. The radiative model for atoms is obtained by grouping elementary levels having similar characteristics; the equivalent spontaneous emission probability of each average level is determined based on the National Institute of Standards and Technology database [52], as shown in [1]. In total, we take into account 45 spontaneous emission lines for N and 24 lines for O. The radiative and dielectronic recombination processes, neglected in the previous analysis given in [1], are added to the model based on the

rate coefficients proposed by Bourdon and Vervisch [22] and Bourdon et al. [23].

As far as molecules are concerned, some states of species mentioned in Table 1 radiate strongly. The $\beta(B^2\Pi \rightarrow X^2\Pi)$ and $\gamma(A^2\Sigma^+ \rightarrow X^2\Pi)$ systems of NO, as well as the first positive $(B^3\Pi_g \rightarrow A^3\Sigma_u^+)$ and second positive $(C^3\Pi_u \rightarrow B^3\Pi_g)$ systems of N_2, and the first negative system $(B^3\Sigma_u^+ \rightarrow X^2\Sigma_g^+)$ of N_2^+, have been considered. Since a vibrational equilibrium is assumed at the species vibrational temperature T_v, the equivalent probability of transition from the electronic state i to state $j < i$ is expressed for these systems as

$$A_{ij} = \frac{\sum_{v'v''} \hat{A}_{v'v''} \exp[-E(v')/k_B T_v]}{\sum_{v} \exp[-E(v)/k_B T_v]} \tag{1}$$

where quantity $\hat{A}_{v'v''}$ stands for the Einstein coefficient for the (v', v'') transition, where $v' > v''$, k_B is the Boltzmann constant, and the symbol $E(v)$ is the vibrational energy of the vth state. In this work, the equivalent transition probabilities A_{ij} have been calculated by fitting the data calculated by Laux and Kruger [53].

The possible reabsorption of radiation is estimated by making use of escape factors. It is assumed here that an optically thin medium is associated with an escape factor equal to one, whereas for an optically thick medium, the escape factor is set to zero.

4. *Master Equation*

In the CR model, the electronic energy relaxation is accounted for by solving electronic master equations based on the different elementary processes mentioned previously. In particular, the chemical rate for the production of an excited atom on the electronic level i, for the processes of excitation and ionization by electron and heavy-particle impact, radiative and dielectronic recombination, spontaneous emission, and absorption, can be written as

$$\begin{aligned}\dot{\omega}_i = &\sum_{j\in\mathcal{A}_i} k^e_{ji} N_j N_e + \sum_{\substack{j\in\mathcal{A}_i \\ l\in\mathcal{H}}} k^l_{ji} N_j N_l + N_e N_{i+}\Bigg[\beta^{e,b}_i N_e + \sum_{l\in\mathcal{H}} \beta^{l,b}_i N_l \\ &+ \alpha^{RR}_i \kappa^{RR}_i + \alpha^{RD}_i \kappa^{RD}_i\Bigg] + \sum_{\substack{j\in\mathcal{A}_i \\ j<i}} \alpha_{ji} A_{ji} N_j - N_i\Bigg[\sum_{j\in\mathcal{A}_i} k^e_{ij} N_e \\ &+ \sum_{\substack{j\in\mathcal{A}_i \\ l\in\mathcal{H}}} k^l_{ij} N_l + \beta^{e,f}_i N_e + \sum_{l\in\mathcal{H}} \beta^{l,f}_i N_l + \sum_{\substack{j\in\mathcal{A}_i \\ j<i}} \alpha_{ij} A_{ij}\Bigg], \qquad i \in \mathcal{A}\end{aligned} \tag{2}$$

where the symbol $\mathcal{A}$ stands for the set of indices for the electronic energy levels of the N and O atoms. The set of indices for companion electronic levels is denoted by $\mathcal{A}_i$. This set is $\mathcal{N}$ for an electronic level of the nitrogen atom and $\mathcal{O}$ for oxygen, with $\mathcal{A} = \mathcal{N} \cup \mathcal{O}$. Symbol $\mathcal{H}$ stands for the set of indices for the heavy particles. Symbol N_i stands for the molar number density of the species or pseudospecies i. The reaction rate constants for excitation k^*, ionization $\beta^{*,f}$, and recombination $\beta^{*,b}$ depends on the collision partner: electron impact interactions are denoted by the superscript e, and heavy-particle impact interactions are denoted by the superscript $l \in \mathcal{H}$. For radiative and dielectronic recombination, effective recombination rate coefficients are introduced as κ^{RR} and κ^{RD}, respectively. The symbol α indicates the escape factor for the radiative process considered: α_{ji} is related to the bound–bound transition from j to i, α^{RD}_i is related to dielectronic recombination, and α^{RR}_i is related to radiative recombination. Subscript $i+$ refers to the ion created when a bound electron of species i is stripped due to kinetic processes. The reverse kinetic processes (i.e., deexcitation and recombination by electron or heavy-particle impact) have been estimated using the detailed balance. The reactions that are not explicitly given in Eq. (2), such as dissociation, exchange, associative ionization, and their reverse processes, are also considered in the model, since they contribute to populate the electronic levels of atoms. They are described by the law of mass action [54].

In a similar manner, the chemical rate for the production of an excited molecule on the electronic level i, for the processes of excitation, ionization, and dissociation by electron and heavy-particle impact, spontaneous emission, and absorption, can be written as

$$\begin{aligned}\dot{\omega}_i = &\sum_{j\in\mathcal{M}_i} k^e_{ji} N_j N_e + \sum_{\substack{j\in\mathcal{M}_i \\ l\in\mathcal{H}}} k^M_{ji} N_j N_l + N_e N_{i+}\Bigg[\beta^{e,b}_i N_e + \sum_{l\in\mathcal{H}} \beta^{l,b}_i N_l\Bigg] \\ &+ N_{i1} N_{i2}\Bigg[\gamma^{e,b}_i N_e + \sum_{l\in\mathcal{H}} \gamma^{l,b}_i N_l\Bigg] + \sum_{\substack{j\in\mathcal{M}_i \\ j<i}} \alpha_{ji} A_{ji} N_j - N_i\Bigg[\sum_{j\in\mathcal{M}_i} k^e_{ij} N_e \\ &+ \sum_{\substack{j\in\mathcal{M}_i \\ l\in\mathcal{H}}} k^l_{ij} N_l + \beta^{e,f}_i N_e + \sum_{l\in\mathcal{H}} \beta^{l,f}_i N_l + \gamma^{e,f}_i N_e + \sum_{l\in\mathcal{H}} \gamma^{l,f}_i N_l \\ &+ \sum_{\substack{j\in\mathcal{M}_i \\ j<i}} \alpha_{ij} A_{ij}\Bigg], \qquad i \in \mathcal{M}\end{aligned} \tag{3}$$

where the symbol $\mathcal{M}$ stands for the set of indices for the electronic energy levels N_2, NO, and O_2 molecules, and the N_2^+, NO^+, and O_2^+ molecular ions. The set of indices for companion electronic levels is denoted by $\mathcal{M}_i$. The excited electronic states of the molecular species undergo dissociation (recombination) due to interaction with the electrons and heavy particles. The corresponding reaction rate coefficients are denoted in Eq. (3) by means of symbols $\gamma^{*,f}_i$ and $\gamma^{*,b}_i$.

The overall number of kinetic and radiative processes exceeds 30 000, which gives an idea of the complexity of the model, as opposed to simplified kinetic mechanisms often used in the literature that do not account for more than 50 kinetic processes.

C. Shock-Tube Flow Solver

In [1], we have developed a 1-D flow solver (shocking), based on [55], to simulate air plasmas obtained in shock-tube facilities. The non-Boltzmann behavior of the electronic energy levels of atoms was accounted for. In the present work, the conservation equations for electronic energy levels of molecules were added to the shocking code with the chemical production rates given in Eq. (3). The separate equation for the free-electron energy/Boltzmann electronic energy adopted in [1], has been combined with the conservation equation for the vibrational energy of the nitrogen molecule.

The newly introduced radiative and dielectronic recombination processes require an associated source term accounting for the loss in free-electron energy due to emission of continuum radiation. These energy losses are modeled as

$$\begin{aligned}Q^{\mathrm{Rad}}_{RR-RD} = &\sum_{j\in\mathcal{N}} (\mathcal{I}_{\mathrm{N}} - E_j) N_e N_{\mathrm{N}^+}\left(\alpha^{RR}_j \kappa^{RR}_j + \alpha^{RD}_j \kappa^{RD}_j\right) \\ &+ \sum_{j\in\mathcal{O}} (\mathcal{I}_{\mathrm{O}} - E_j) N_e N_{\mathrm{O}^+}\left(\alpha^{RR}_j \kappa^{RR}_j + \alpha^{RD}_j \kappa^{RD}_j\right)\end{aligned} \tag{4}$$

where $\mathcal{I}_{\mathrm{N}}$ and $\mathcal{I}_{\mathrm{O}}$ are the ground atomic state ionization energy for atomic nitrogen and oxygen, respectively.

III. Results

In this work, we investigate the behavior of the electronic energy level populations of the atoms and molecules for the trajectory point

Table 2 Shock-tube flow characteristic quantities

Parameter	Value
Time	1634 s
p_1	2 Pa
T_1	195 K
u_1	11,360 m/s
p_2	3827
T_2	62,377 K
u_2	1899 m/s

of the FIRE II experiment at 1634 s by using the full ABBA CR model. The set of operating conditions for the corresponding shock-tube problem are given in Table 2. Freestream characteristic quantities are denoted by the subscript 1, and postshock characteristic quantities are denoted by subscript 2. The symbol u stands for the flow velocity, p stands for the pressure, and T stands for the translational temperature. The mole fractions of nitrogen and oxygen are assumed to be constant through the shock ($x_{N_2} = 0.79$ and $x_{O_2} = 0.21$). After the shock, the rotational temperature is assumed to be equal to the postshock gas temperature T_2, whereas the vibrational and electron temperatures are still equal to the freestream gas temperature T_1.

A. Comparison of Results Obtained by Means of Full And Atomic ABBA Models

In this section, we compare the results obtained by means of the atomic ABBA model described in [1] and the full ABBA model. The main difference among the two models deals with the treatment for the electronic energy level populations of the molecular species. The atomic ABBA model relies on a Boltzmann distribution to describe these populations, as opposed to the full ABBA model for which a state-specific treatment is preferred. In both CR models, we use Park's model [12] for dissociation and a nonpreferential dissociation model for the vibration-dissociation coupling.

Figure 1a shows the evolution of the temperature profiles obtained by means of the full ABBA model, and Fig. 1b shows the profiles obtained by means of the atomic ABBA model. The thermal relaxation distance for the rotranslational temperature is found to be larger for the full model: thermal equilibrium is obtained after a distance of 2.5 cm from the shock, as opposed to a distance of 1.5 cm for the atomic model. Furthermore, vibrational temperatures computed using the full model exhibit a less pronounced overshoot with respect to the atomic model. We have checked that this overshoot is due to the absence of the preferential dissociation model for the chemistry-vibration coupling and the use of the Landau–Teller formula, without Park's correction [12] in the atomic CR model. Johnston [4] has found that thermal equilibrium is reached after a distance of 1.8 cm from the shock, and the postshock rotranslational temperature and vibrational-electronic temperature, based on the shock-slip condition, are different from the temperatures that we have computed based on the Rankine–Hugoniot relations. The shock-slip equations contain conduction and diffusion terms that are not present in the Rankine–Hugoniot equations. As a consequence, the values of the vibrational temperatures are significantly larger than the freestream temperature when the shock-slip conditions are employed. Finally, we have verified that the results presented in this paper are rather insensitive to the temperature differences in the narrow region close to the shock front. In a future work, a global sensitivity analysis of the model would be of interest to quantify this effect.

Figures 2a and 2b compare the evolution of the species number densities computed in the postshock area by means of by the full and atomic ABBA models, respectively. We note a similar evolution for most species, except for N_2^+. The N_2^+ number density computed based on the full model exhibits an overshoot right after the shock, as opposed to a slow increase toward an equilibrium value, predicted by means of the atomic model. The reason for this disagreement is due to

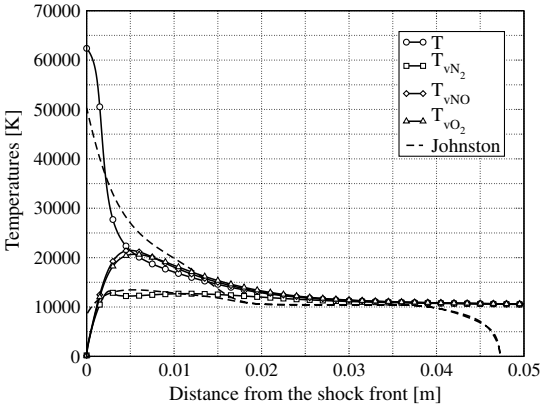

a) Full ABBA model (solid lines) and Johnston's results [4] (dashed lines)

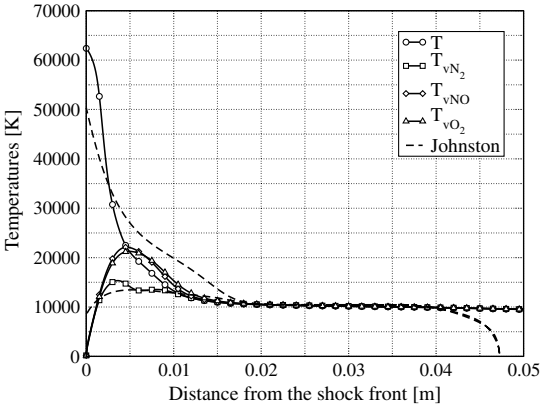

b) Atomic ABBA model (solid lines) and Johnston's results [4] (dashed lines)

Fig. 1 Temperature profiles for FIRE II test case at 1634 s using different CR models.

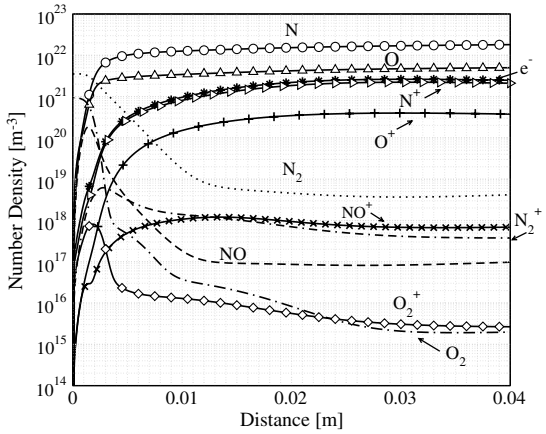

a) Full ABBA model

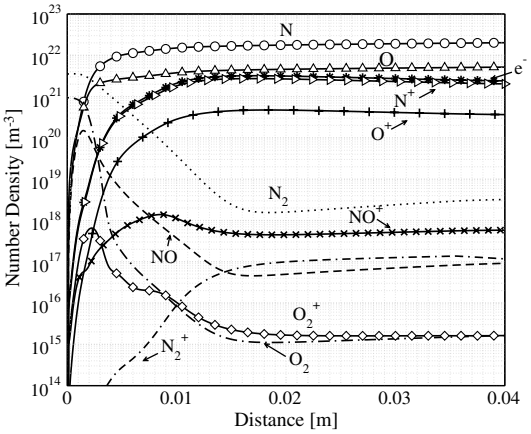

b) Atomic ABBA model

Fig. 2 Density profiles for FIRE II test case at 1634 s using different CR models.

the differences in the kinetic mechanism used for the reaction rate coefficients. A thorough analysis of the experimental results of Grinstead et al. [56] shows an overshoot in the radiation from the $N_2^+(1-)$ system and suggests the presence of an overshoot in the N_2^+ population. It is interesting to note that the simulations carried out by Johnston [4] also confirm the presence of an overshoot in the population of the excited states after the shock.

B. Detailed Physicochemical Analysis of Results Obtained by Means of Full ABBA Model

In this section we first we present the evolution of electronic states of molecular species through the shock layer. We focus on N_2^+ and N_2, since both molecules contribute to the nonequilibrium radiative signature of the gas under high-speed reentry conditions. We have checked that the contributions from the NO and O_2 bands are limited, since at these high temperatures are found to be almost completely dissociated. Second, we analyze the influence of the modeling of dissociation, radiation, and ionization on the distribution function of atomic nitrogen. All these effects are believed to affect the physicochemical properties of the plasma in the shock layer. Hence, in this section, we try to have a quantitative idea (when possible) of their effective influence on the electronic excitation of the atoms.

1. N_2^+ and N_2 Number Density Profiles

Figure 3a shows the number density profiles for the ground and excited electronic states of N_2^+ for an optically thin medium, compared with their equilibrium value. All the electronic energy levels of the N_2^+ molecule are found to be in equilibrium, confirming the prediction of [4]. At speeds up to 10 km/s, N_2^+ is a strong radiator in the UV range of the spectrum, due to the bound transitions from $N_2^+(B^2\Sigma_u^+)$ to $N_2^+(X^2\Sigma_g^+)$. In this work, we have checked that the population of the radiative $B^2\Sigma_u^+$ state is governed by transitions to and from the ground state due to electron impact. It is interesting to note that the $B^2\Sigma_u^+$ state can also be formed through a very efficient process known as inverse predissociation [12]. We have checked that inverse predissociation is of secondary importance for the population of the $B^2\Sigma_u^+$ state when compared with excitation by electron impact.

Figure 3b shows the number density profiles for the ground and excited electronic states of N_2 for an optically thin medium, compared with their equilibrium value. The $N_2(A^3\Sigma_u^+)$ and $N_2(B^3\Pi_g)$ states, close in energy, are shown to have similar evolutions and very close values of number densities in the shock layer. Departures of the excited electronic energy level populations from equilibrium are located close to the shock front, where the peak for the population is less sharp for the non-Boltzmann calculation than for the equilibrium prediction.

2. Influence of Dissociation Model on Results

The mechanism for production of free electrons is governed by the associative ionization reaction and, to a lesser extent, by the direct ionization of the atomic species. Both processes depend on the production of atomic species by dissociation. Therefore, in this section, we carry out a sensitivity analysis of our results on the models used to describe dissociation.

Figures 4a and 4b show the evolution of the temperatures in the postshock region for the Macheret–Fridman and Treanor–Marrone

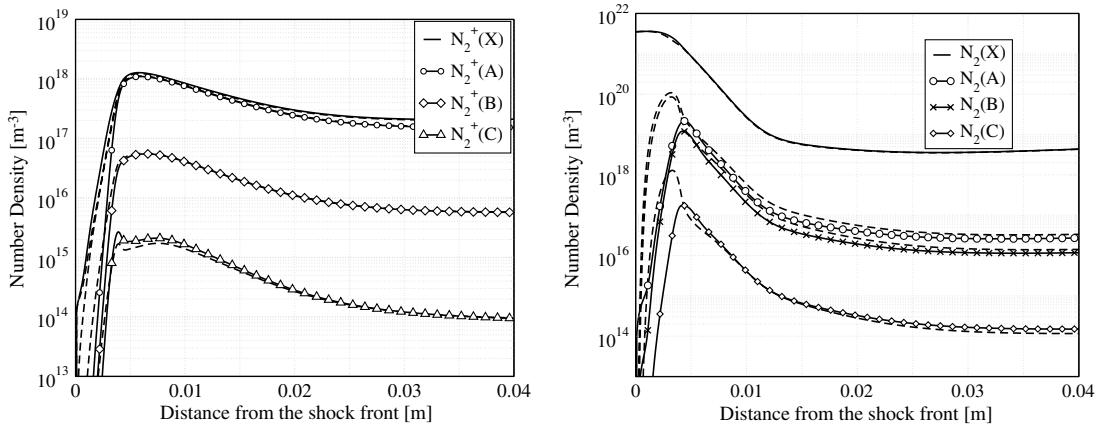

a) N_2^+ b) N_2

Fig. 3 Electronic energy level population profiles for N_2^+ and N_2 molecules for FIRE II test case at 1634 s (dashed lines: equilibrium densities; solid lines: full ABBA model)

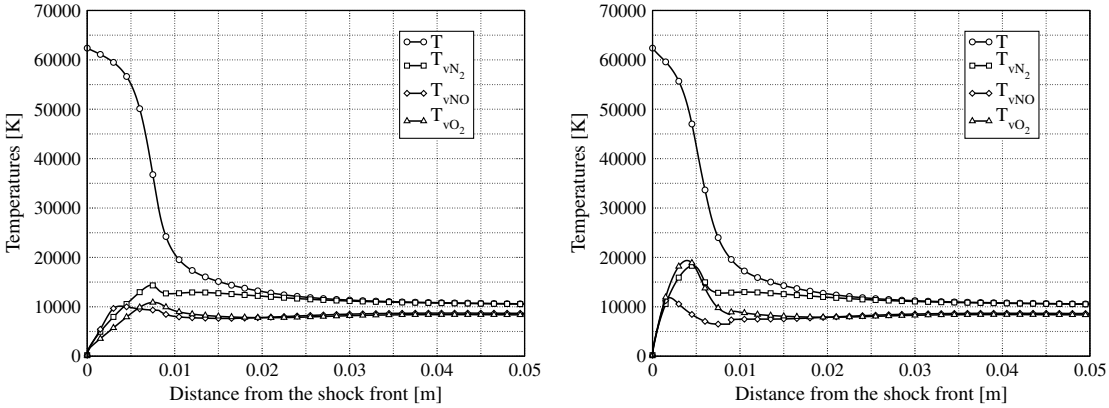

a) Macheret model b) Treanor-Marrone model [41] with $U = T_D/3$ (equivalent dissociation temperature)

Fig. 4 Influence of dissociation models on temperature profiles for FIRE II test case at 1634 s, full ABBA model.

models presented in Sec. II, respectively. The thermal behavior through the shock layer is very similar for these two models, but it strongly differs from the prediction shown in Fig. 1a, obtained by means of the following reference model: the full ABBA model with Park's model [12] for dissociation. The main difference lies in the absence of overshoot for the NO and O_2 vibrational temperatures. The reason for such a difference can be explained by the preferential dissociation assumption for the vibration-dissociation coupling in the Treanor–Marrone or Macheret–Fridman models, as opposed to the nonpreferential assumption in the reference model. Thus, by allowing the molecules to dissociate at higher vibrational levels, the energy removal due to dissociation processes exceeds the average vibrational energy and tends to lower the postshock vibrational temperatures. In practice, the magnitude of the source term for chemistry-vibration coupling is higher for the preferential dissociation models than the corresponding source term for the nonpreferential dissociation model.

Figure 5a shows the number density profiles for the N_2, O_2, NO, and N_2^+ molecular species for the three different dissociation models used in this work. The models based on the preferential dissociation predict the same evolution for the composition of these molecular species, as shown in Fig. 5a. As expected, some differences are observed when these results are compared with the ones based on the nonpreferential dissociation model, which predicts a faster dissociation of the molecules. The models proposed by Marrone and Treanor [41] and Macheret et al. [37] introduce a delay in the production of the free electrons and then a slight displacement of the peak in the electron density, as shown in Fig. 5b.

In conclusion, although preferential dissociation models lead to a less effective dissociation of the molecules and to lower vibrational energies through the shock layer, such effects are small for the analyzed flow conditions. Hence, we have used a nonpreferential dissociation model in the subsequent analysis.

3. *Influence of Optical Thickness and Ionization Precursor on Results*

In the previous sections, we have assumed that the gas is optically thin. Thus, all the radiation emitted in the shock layer is not reabsorbed by the gas in the computational domain: there is no interaction between the emitted radiation and the atoms and molecules. In this section, we propose to study the influence of the optical thickness of the medium on the population of the excited electronic states of the atomic species by changing the value for the escape factors of some atomic lines. It is well known that the resonance lines tend to be self-absorbed, affecting the internal energy distribution function of atomic nitrogen and oxygen. To account for this phenomenon, the escape factors of the vacuum UV (VUV) lines are set to zero, and for the other radiative transitions, they are set to one. The results are shown in Fig. 6a for the electronic energy populations of nitrogen atoms. The low-lying excited states (strongly radiating in the VUV

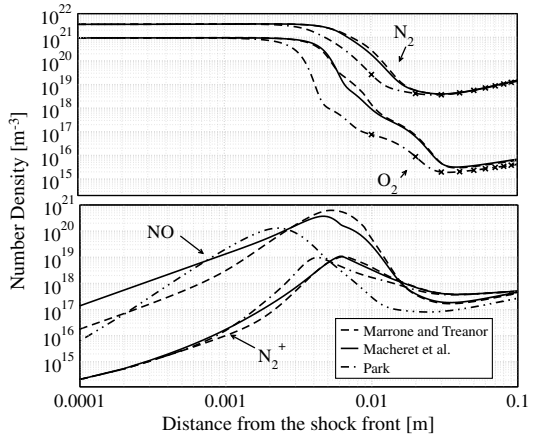

a) N_2, O_2, NO, and N_2^+: Treanor-Mallone model [41] (dashed lines); Macheret-Fridman model [37] (solid lines); and Park's model [12] (dotted-dashed lines)

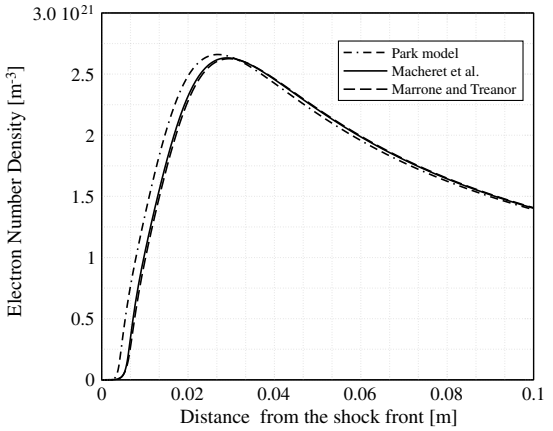

b) Free electrons : Treanor-Mallone model [41] (dashed lines); Macheret-Fridman model [37] (solid line); and Park's model [12] (dotted-dashed line)

Fig. 5 Influence of dissociation models on species number density profiles for FIRE II test case at 1634 s, full ABBA model.

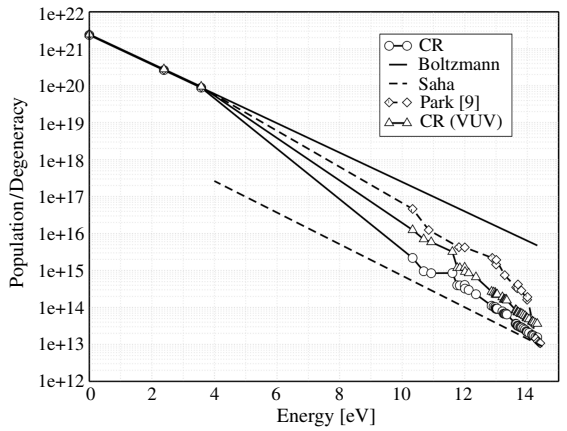

a) Electronic energy level populations for atomic nitrogen at 1 cm from the shock front; Park's model (◇); ABBA model with $\alpha = 1$ (○); ABBA model with self-adsorbed vuv lines (△)

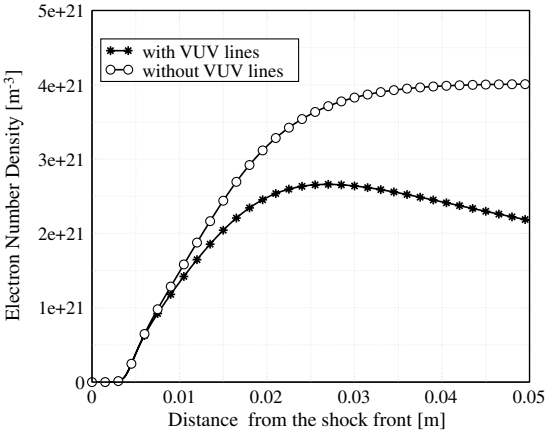

b) Electron density profiles; ABBA model with $\alpha = 1$ (*) ; ABBA model with self-adsorbed vuv lines (○)

Fig. 6 Influence of optical thickness on population profiles of species for FIRE II test case at 1634 s.

part of the spectrum) are found to be overpopulated with respect to the results obtained by assuming an optically thin gas. Then, when self-absorption of the VUV lines is considered, a better agreement is observed with the results obtained by using Park's model [9,10]. Furthermore, Fig. 6b shows that the electron number density evolution is strongly affected by the optical thickness of the gas. For an optically thin medium, the profile of the electron density presents a maximum followed by a monotonic decrease. When self-absorption of the VUV lines is considered, the electron number density increases monotonically and reaches a plateau region. This behavior is due to radiation cooling, which removes energy from the flow, thus lowering the temperature of the free electrons that recombine. The influence of radiation on the ionization degree of low-temperature plasmas was discussed in detail in [57].

As radiation is emitted in the shock layer, part of it may propagate ahead of the shock and be reabsorbed by the cold gas. Such an interaction produces ionization, dissociation, and excitation of the internal energy modes of the gas particles ahead of the shock. Accurate modeling of these phenomena, known as precursor effects, would require us to fully couple radiative heat transfer and flow solvers. This topic is out of the scope of this paper, where a simple approach is used to estimate the amount of electrons just after the shock, allowing us to study the importance of precursor effects.

Gorelov et al. [58] have analyzed a large number of experiments in shock tubes and found the dependence of the ionization density as a function of the shock speed and pressure. The results of such analysis are summarized in Fig. 7 (taken from [58]), which describes the measured electron densities as a function of the distance ahead of the shock wave. On the same figure, a comparison with theory is shown and a fairly good agreement with experiments is observed. The shock conditions studied in the present work are close to those studied by Gorelov et al. Then, to estimate the influence of precursor electrons on our results, we have chosen an electron density of 10^{19} m^{-3}, which corresponds to the maximum value of the electron density in Fig. 7. We have also assumed that the temperature of free electrons is about 8000 K in order to maximize the precursor effects.

Figure 8 presents the electronic energy level populations for atomic nitrogen at 1 cm from the shock front, with and without precursor electrons. We note that the presence of the free electrons ahead of the shock slightly increases the populations of atomic nitrogen electronic energy levels. For the shock conditions studied in this paper, the effects of precursor electrons is found to be negligible.

4. *Influence of Heavy-Particle Impact Excitation Processes on Ionization*

Ionization by electron impact is a ladder-climbing process, in which the atoms are first electronically excited and ionize when they are close enough to the ionization limit. In fact, since in our case, the kinetic energy of the free electrons is much smaller than the ionization potential, i.e., ($\mathcal{I} \gg kT_e$) (where $\mathcal{I}$ is the ground atomic state ionization energy), the atomic ionization occurs mainly from the upper excited states with the ionization energy equal to ($\mathcal{I} - kT_e$). Therefore, ionization processes are strongly affected by the populations of electronic states.

In the present section, we investigate the influence of the inelastic collisions among heavy particles on the ionization process. It is commonly believed that the excitation of electronic energy modes of atoms is dominated by the interaction with free electrons [12,59], except right after the shock where the electron density is scarce, and then excitation is due to collisions with molecules [54,60].

Figure 9 shows the effect of the individual processes on the electron number density profile. We note that heavy-particle excitation and ionization processes have a significant impact on the electron density profile just after the shock but have no influence at 1 cm and downstream of the shock. In fact, heavy-particle excitation and ionization processes contribute to the formation of the first electrons in the postshock region. In particular, the processes involving molecular species tend to produce electrons close to the shock, as opposed to the atoms that can contribute to the formation of the electrons only when a significant amount of dissociation has taken place. However, the amount of electrons produced by heavy-particle excitation and ionization processes close to the shock is fairly small. If we compare the electron density produced by the interaction with the heavy particles with Fig. 7, we can see that the radiation emitted in the shock layer that interacts with atoms and molecules in the preshock region produces more electrons than heavy-particle inelastic processes. Therefore, the importance of the heavy-particle

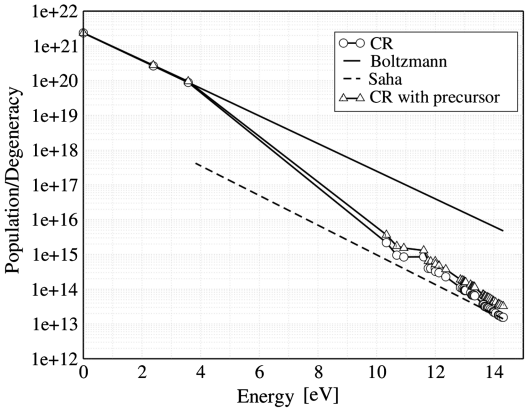

Fig. 8 Electronic energy level populations for atomic nitrogen at 1 cm from the shock front. ABBA model with $\alpha = 1$ and no precursor electrons (○), ABBA model with $\alpha = 1$ and with precursor electrons (△), Boltzmann equilibrium (solid line), and Saha equilibrium (dashed line).

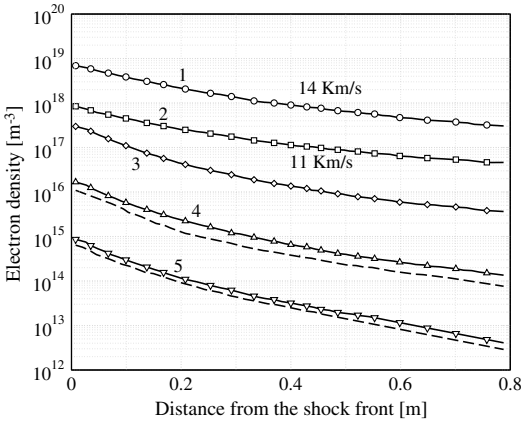

Fig. 7 Electron population distributions ahead of a shock wave. Freestream pressure $p1 = 0.2$ torr: $1 - u_1 = 14.0$ km/s and $2 - u_1 = 11.3$ km/s; freestream pressure $p1 = 0.5$ torr: $3 - u_1$, =9.5 km/s, $4 - u_1 = 7.5$ km/s, and $5 - u_1 = 6.0$ km/s; and dashed lines: calculated results. Experimental and calculated results taken from [58].

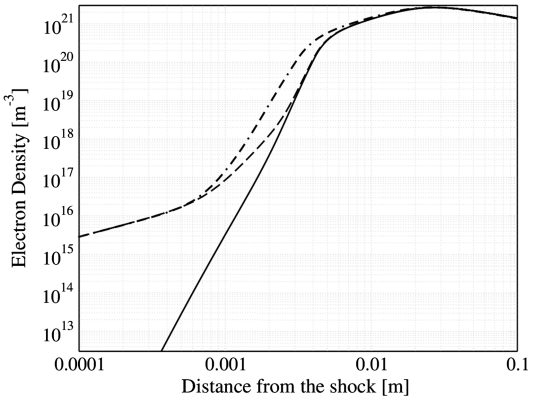

Fig. 9 Electron density profiles. Solid line: only inelastic interactions with electrons (i.e., excitation and ionization) considered; dashed line: inelastic collisions with molecules and electrons; and dotted–dashed line: all inelastic processes with light and heavy particles considered.

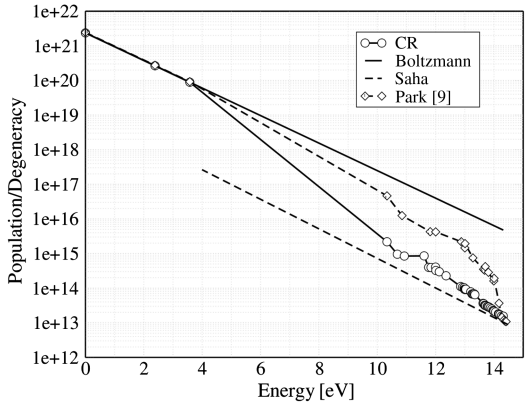

Fig. 10 Electronic energy level populations for atomic nitrogen at 1 cm from the shock front. Park's model (◇), ABBA model with $\alpha = 1$ (○), Boltzmann equilibrium (solid line), and Saha equilibrium (dashed line).

excitation processes is reduced if the interaction of the radiative field and the flowfield is correctly accounted for.

C. Comparison of Full ABBA Model with Park's Model

In this section, we present a comparison between the full ABBA model and the CR model recently developed by Park [9,10] and Hyun et al. [11]. Besides the differences in the models used for the molecular and atomic elementary processes, the two CR models differ in the way they deal with the time integration and the coupling of the CR model with the flow. Our CR model is time dependent and fully coupled with the equations of the 1-D shock. Park's model [9,10], as it is implemented in the SPRADIAN code, assumes that the QSS condition is reached for the excited states and solves a nonlinear algebraic set of equations. Furthermore, SPRADIAN is used in postprocessing, totally decoupled from the flowfield calculation. Influences of such assumptions on the results have been thoroughly studied in [1] for the atomic ABBA model.

To compare our results with those obtained with Park's model [9,10], we use as reference calculations the results obtained with the full ABBA model assuming an optically thin medium. From these results, we extract flowfield quantities, such as temperatures and composition of the different species, obtained by summing the concentrations of all the electronic states of the full ABBA model. The flowfield quantities are then used as input into the SPRADIAN code to predict the nonequilibrium populations of the excited states of molecules and atoms.

Figure 10 shows the electronic level population of nitrogen atoms at 1 cm from the shock front. We note that in both models, the populations of the ground state [N(^4S)] and the two metastable states [N(^2D) and N(^2P)] are found to be in Boltzmann equilibrium. Both models also predict a depopulation of high-lying excited states in comparison with a Boltzmann distribution. However, the populations of the upper levels ($E > 10$ eV) calculated with Park's model [9,10] are about one order of magnitude larger than those calculated with the full ABBA model. We note that, for levels close to the ionization limit, a Saha equilibrium is obtained with the full ABBA model.

The perturbation of the electronic energy distribution function is confirmed by an analysis of the radiative heat flux measurements performed during the reentry phase. The values of the heat flux were found to be much lower than the predictions [12,61] made before flight. Such predictions were based on the assumption of a Boltzmann distribution for the populations of excited states. When departures from Boltzmann equilibrium are accounted for, excellent agreement with the experimental values is found [4]. The strong depopulation of the excited states (Fig. 10) drastically influences the radiative signature of the gas, which is dominated by atomic line radiation at these flight conditions.

As the vehicle approaches the lower parts of the atmosphere, the pressure rises and the importance of the collision processes with respect to the radiative processes begins to increase. This is due to the collisional processes scaling with p^2, as opposed to the radiative effects that scale with p. In the lower parts of the atmosphere, the distributions are found to be Boltzmann, as shown in [1].

Figures 11a and 11b compare the populations of excited states of the molecular species calculated with Park's model [9,10] and the full ABBA model. For N_2^+, it is important to note that Park's model includes the D state of N_2^+ and does not consider the C state. Figure 11a shows that, for N_2^+, the two models are in good agreement, and then, as was shown in Fig. 3a, the populations of the three first excited electronic states are in equilibrium. Conversely, Fig. 11b shows discrepancies between both models for the concentration of the excited states of the N_2 molecules. Park's model predicts a sharp overshoot of the population of the excited levels approaching the equilibrium values (Fig. 3b), while our results show a smoother relaxation toward the equilibrium region.

In conclusion, the comparison of the results obtained with the full ABBA model and the recent model of Park [9,10] shows a rather good agreement for air molecules and more significant discrepancies for the populations of the electronic levels of air atoms.

D. Derivation of Reduced Kinetic Mechanism: Simplified ABBA Model

The analysis of the results presented in Secs. III.B and III.C for the atomic species suggests the possibility of reducing the number of levels to be considered in the CR model by grouping the high-lying

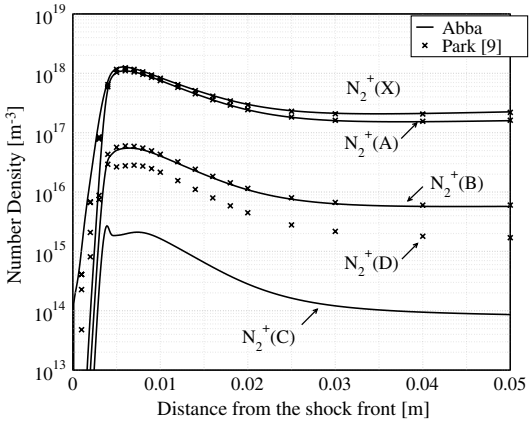

a) Population profiles of N_2^+ molecular ions: Park's CR model (×); full ABBA model (solid lines) (note: Park's model includes the D state of N_2^+ and does not consider the C state)

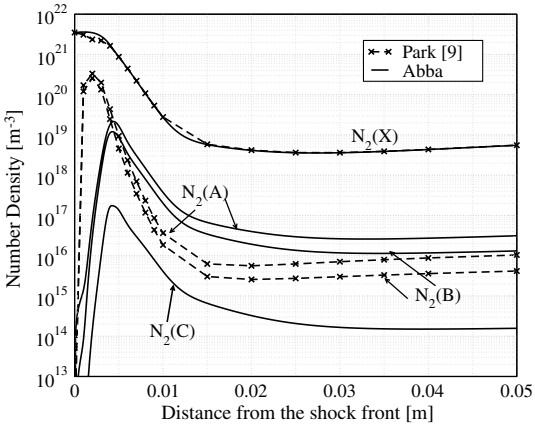

b) Population profiles of N_2 molecules: Park CR model (×); full ABBA model (solid lines)

Fig. 11 Comparison of population profiles of N_2^+ and N_2 molecules obtained with Park's CR model [9] and the full ABBA model.

Table 3 Grouped states in the simplified ABBA model for N and O atoms

Grouped states	States of N	Energy, eV	States of O	Energy, eV
1	1	0.	1	0.
2	2	2.38	2	1.97
3	3	3.58	3	4.19
4	4–6	10.69	4–6	9.52
5	7–13	12.	7–13	12.09
6	14–21	12.98	14–21	12.78
7	22–27	13.27	22–27	13.05
8	28–46	13.68	28–40	13.464

excited levels of N and O atoms. Indeed, many electronic levels, owing to a reduced energy spacing, are likely to be in equilibrium among each other due to an efficient collisional coupling. Furthermore, the levels located very close to the continuum are in chemical equilibrium (Saha equilibrium) with the free electrons, and their populations can be easily estimated by means of the Saha equation. Therefore, the description of the detailed kinetic processes for these electronic states results in an increase of the computational effort without improving the accuracy of the model. However, it is important to note that low-energy metastable states have a substantially different behavior from the high-lying excited states [14]. Then, the different dynamics of the kinetics of the metastable and high-lying excited states require a separate grouping. Furthermore, among the high-lying excited states, we can distinguish two groups of levels: those close to the ionization limit, which do not radiate significantly and are in Saha equilibrium, and the lower excited levels close to the metastable states, which strongly radiate in the VUV region of the spectrum and are less efficiently coupled by collisions, owing to the larger energy barrier between them. Then, the three macroscopic groups of levels have been subdivided, as detailed in Table 3. The ground and the metastable states are not grouped together, since as observed in [1], their populations may depart from the Boltzmann distribution. Furthermore, an accurate estimation of their population is crucial, since they are highly populated and strongly contribute to the excitation of the upper states [62,63]. For the second macroscopic group of levels, an important constraint to be considered is given by the radiative transitions: in order to preserve the role played by radiation on the populations of the levels, it is important to avoid the grouping of two levels that interact through major radiative transition processes [64]. Then, finally, three grouped states have been considered in the second macroscopic group of levels. For the third macroscopic group of levels corresponding to high-energy levels in Saha equilibrium, two grouped states have been considered.

1. *Elementary Processes of Grouped Levels*

To model the plasma with the reduced model, we have to determine the rates of collisional and radiative processes of the grouped levels based on rates of elementary processes between ungrouped states. In this work, to determine the rates of excitation and ionization processes for the grouped levels, we propose to average the rates of elementary processes between ungrouped levels, assuming that these levels follow a Boltzmann distribution. The same type of averaging is required for the inelastic excitation involving heavy particles. However, given their reduced influence on the excitation as well as the ionization processes, such induced processes have been neglected.

For radiative processes, it is important to note that radiative processes within the same grouped level have been discarded, since they do not affect the population of the level. In principle, we could account for their contribution to the radiation cooling; however, given the low-energy content, such contribution was considered negligible.

a. Ionization Rate Coefficients of Grouped Levels. The ionization rate coefficient from the Lth grouped level is obtained by averaging the rates of each ungrouped state over the Boltzmann distribution. Therefore, $\mathcal{K}_f^{L\to c}$, the averaged ionization rate coefficient from the Lth grouped level, is given by

$$\mathcal{K}_f^{L\to c} = \sum_i^{N_L} \frac{N_i}{N_{\mathrm{TOT}}} k_{i,f}^{i\to c} \tag{5}$$

where N_L indicates the number of levels included in the lumped group, N_{TOT} is the total number density of the lumped level, and $k_{i,f}$ refers to the rate constant for electron impact ionization of the single state.

Substituting the Boltzmann distribution function into Eq. (5), we obtain

$$\mathcal{K}_f^{L\to c} = \frac{\sum_i^{N_L} g_i k_{i,f}^{i\to c} \exp(-E_i/k_B T_e)}{\sum_k^{N_L} g_k \exp(-E_k/k_B T_e)} \tag{6}$$

b. Excitation Processes for Grouped Levels. Indicating with L^* the initial grouped level and with L^{**} the final grouped state, the averaged rate constant for the $L^* \to L^{**}$ transition with $L^* < L^{**}$ reads

$$\mathcal{K}_f^{L^*\to L^{**}} = \sum_i^{N_{L^*}} \frac{N_i}{N_{\mathrm{TOT}}^*} \sum_j^{N_{L^{**}}} k_f^{i\to j} \tag{7}$$

where N_{TOT}^* is the number density of the initial grouped state L^*. The indices i and j indicate, respectively, the ungrouped states of the lower and upper excited states, L^* and L^{**}, respectively. The rate coefficient for the electron impact excitation from the generic level i to the level j is indicated with $k_f^{i\to j}$. Assuming the Boltzmann population of the grouped states, Eq. (7) becomes

$$\mathcal{K}_f^{L^*\to L^{**}} = \frac{\sum_i^{N_{L^*}} \sum_j^{N_{L^{**}}} g_i k_f^{i\to j} \exp(-E_i/k_B T_e)}{\sum_k^{N_L^*} g_k \exp(-E_k/k_B T_e)} \tag{8}$$

In a similar manner, the excitation rate constants from the ground and the metastable states to the lumped states (indicated with L) are estimated by

$$\mathcal{K}_f^{i\to L} = \sum_j^{N_L} k_f^{i\to j} \tag{9}$$

Where i represents the index of the ground, first, or second metastable state for nitrogen or oxygen atoms.

The reverse rates based on detailed balance are a function of the averaged forward rates presented in this section and on the equilibrium constants for the grouped states [54].

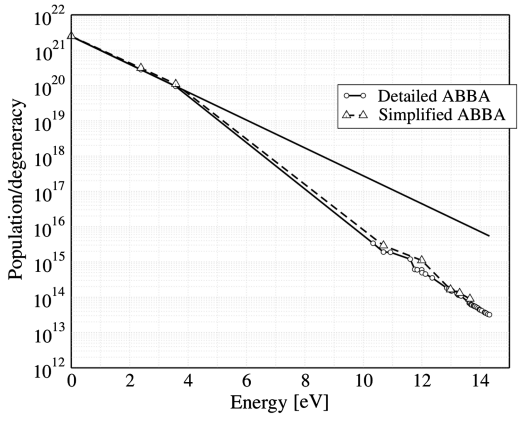

Fig. 12 Electronic energy level populations for atomic nitrogen at 1 cm from the shock front. Detailed ABBA model (○); and simplified CR approach (△).

2. Comparison Between Approximate and Detailed Collisional-Radiative Model

The validation of the reduced CR model is obtained by comparing the electronic distribution function given by the approximate model with the one obtained with the detailed CR model. In this section, the detailed CR model accounts for neutral and charged species and includes a detailed treatment of the electronic states of nitrogen, N(1–8), and oxygen, O(1–8), atoms, whereas the molecular species are assumed to be populated according to Boltzmann distribution. The comparison between the two CR models is performed analyzing the Boltzmann diagrams at 1 cm from the shock front for the shock conditions of Table 2.

Figure 12 shows the populations of the atomic nitrogen levels for the two models. We note that differences are limited to a small departure in the population density in the intermediate-energy range. High-lying excited states close to the continuum, as well as the metastable states, are very well described by the few states of the simplified model. To improve the agreement among the intermediate states, the number of grouped levels could be increased, increasing the accuracy but also computational time. Computational efficiency of the model is easily demonstrated if we consider that a full simulation with the reduced models requires only a couple of seconds, as opposed to the full model that requires about 5 min.

In conclusion, we have shown that to predict the non-Boltzmann electronic distribution of air atoms for high-speed reentry applications, the eight grouped levels for nitrogen and oxygen (listed in Table 3) can substitute the 46 and 40 levels for nitrogen and oxygen, respectively. The derivation of reduced models is very important to improve the accuracy of simplified kinetic mechanisms in 2-D and 3-D flow solvers. Then, this work can be considered as a first step toward the derivation of a new reduced kinetic mechanism for atoms and molecules in air based on the full ABBA CR model.

IV. Conclusions

In this work, the behavior of the excited electronic states of atoms and molecules in the relaxation zone of 1-D air flows obtained in shock-tube facilities has been studies. A CR model has been developed, accounting for thermal nonequilibrium between the translational energy mode of the gas and the vibrational energy mode of individual molecules. The electronic states of atoms and molecules are treated as separate species, allowing for non-Boltzmann distributions of their populations. This CR model has been applied to the study of shock-tube operating conditions corresponding to an early trajectory point of the FIRE II flight experiment with significant nonequilibrium effects.

In the rapidly ionizing regime behind strong shock waves, the electronic energy level populations depart from Boltzmann distributions, since the high-lying bound electronic states are depleted. To quantify the extent of this nonequilibrium effect, the results obtained by means of the CR model were compared with those based on Boltzmann distributions. Conversely to atoms, for the molecules, departures from the Boltzmann equilibrium are limited to a narrow zone close to the shock front. A comparison with the recent model of Park [9,10] reveals an adequate agreement for predictions involving molecules, as opposed to the predictions involving the populations of the electronic levels of atoms that show significant discrepancies.

In this paper, a detailed analysis of the results obtained to understand the relative importance of different physical phenomena occurring in the shock layer of a spacecraft at high reentry speed has been carried out. The influence of the vibration-dissociation coupling is found to have a small influence on the results, because at high speed, the dissociation does occur from all the vibrational levels and is not restricted to the upper vibrational levels. In other words, there is no preferential way for the molecules to dissociate. The influence of the optical thickness on the results puts forward the need for a coupling of radiation and flowfield calculation, given the importance of the radiative processes on the electron energy distribution function and on the thermophysical properties of the plasma. This would allow accounting for precursor phenomena in a physically consistent manner and having a more reliable estimation of the influence of such processes on the thermophysical state of the shock layer. According to approximate estimations, however, it seems that precursor phenomena has little influence on the results.

Finally, in this work, a detailed CR model coupled to a 1-D flow solver has been used. It is unrealistic to implement this detailed model in 2-D or 3-D flow solvers directly. Therefore, a reduced kinetic mechanism has been derived by grouping high-lying excited states of atoms. The accuracy of this model has been demonstrated for the flow conditions studied in this work. In the future, it would be interesting to develop a new reduced kinetic mechanism for air that could be easily used in a wide range of flow conditions by grouping some excited states of atoms and molecules in the full ABBA CR model.

Acknowledgment

The authors would like to acknowledge A. Munafó (diploma course student, von Kármán Institute) for his practical help on the study of dissociation.

References

[1] Panesi, M., Magin, T., Bourdon, A., Bultel, A., and Chazot, O., "Analysis of the FIRE II Flight Experiment by Means of a Collisional Radiative Model," *Journal of Thermophysics and Heat Transfer*, Vol. 23, No. 2, 2009, pp. 236–248. doi:10.2514/1.39034

[2] Bultel, A., Chéron, B., Bourdon, A., Motapon, O., and Schneider, I., "Collisional-Radiative Model in Air for Earth Re-Entry Problems," *Physics of Plasmas*, Vol. 13, No. 4, 2006, pp. 1–11.

[3] Surzhikov, S., "Electronic Excitation in Air and Carbon Dioxide Gas," *RTO-EN-AVT-162 VKI Lecture Series*, Vol. 1, No. 1, NATO, 2008, pp. 1–117.

[4] Johnston, C. O., "Nonequilibrium Shock-Layer Radiative Heating for Earth and Titan Entry," Ph.D. Thesis, Virginia Polytechnic Inst. and State Univ., Blacksburg, VA, 2006.

[5] Surzhikov, S., Rouzaud, O., Soubrie, T., Gorelov, V., and Kireev, A., "Prediction of Non-Equilibrium and Equilibrium Radiation for Reentry Conditions," AIAA Paper 2006-1188, Jan. 2006.

[6] Park, C., "Thermochemical Relaxation in Shock Tunnels," *Journal of Thermophysics and Heat Transfer*, Vol. 20, No. 4, 2006, pp. 689–698. doi:10.2514/1.22719

[7] Park, C., "Review of Chemical-Kinetic Problems of Future NASA Mission, I: Earth Entries," *Journal of Thermophysics and Heat Transfer*, Vol. 7, No. 3, 1993, pp. 385–398. doi:10.2514/3.431

[8] Cauchon, D. L., "Radiative Heating Results from FIRE II Flight Experiment at a Reentry Velocity of 11.4 km/s," NASA Ames Research Center TM X-1402, Moffett Field, CA, 1967.

[9] Park, C., "Rate Parameters for Electronic Excitation of Diatomic Molecules: Electron-Impact Processes," AIAA Paper 2008-1207, Jan. 2008.

[10] Park, C., "Rate Parameters for Electronic Excitation of Diatomic Molecules: Heavy Particle-Impact Processes," AIAA Paper 2008-1206, Jan. 2008.

[11] Hyun, S. Y., Park, C., and Chang, K. S., "Rate Parameters for Electronic Excitation of Diatomic Molecules, III. CN Radiation Behind a Shock Wave," AIAA Paper 2008-1276, Jan. 2008.

[12] Park, C., *Nonequilibrium Hypersonic Aerothermodynamics*, Wiley, New York, 1989, pp. 1–358.

[13] Bates, D., Kingston, A., and McWhirter, R., "Recombination Between Electrons and Atomic Ions. I. Optically Thin Plasmas," *Proceedings of the Royal Society of London, Series A*, Vol. 267, No. 1330, 1962, pp. 297–312. doi:10.1098/rspa.1962.0101

[14] Gorse, C., Cacciatore, M., and Capitelli, M., "Some Aspects in Recombining Transient Nitrogen Plasmas," *Zeitschrift fuer Naturforschung*, Vol. 33a, 1978, pp. 895–902.

[15] Cacciatore, M., and Capitelli, M., "Population Densities and Ionization Coefficient of Fast Transient Hydrogen Plasmas," *Zeitschrift fuer Naturforschung*, Vol. 33a, 1975, pp. 895–902.

[16] Cacciatore, M., and Capitelli, M., "The Temporal Evolution of Population Densities of Excited States in Atomic Oxygen Thin Plasmas," *Journal of Quantitative Spectroscopy and Radiative Transfer*, Vol. 16, No. 4, 1976, pp. 325–334. doi:10.1016/0022-4073(76)90014-5

[17] Colonna, G., Armenise, I., Bruno, D., and Capitelli, M., "Reduction of State-to-State Kinetics to Macroscopic Models in Hypersonic Flows," *Journal of Thermophysics and Heat Transfer*, Vol. 20, No. 3, 2006, pp. 477–486. doi:10.2514/1.18377

[18] Colonna, G., Pietanza, L.-D., and Capitelli, M., "Recombination-Assisted Nitrogen Dissociation Rates Under Nonequilibrium Conditions," *Journal of Thermophysics and Heat Transfer*, Vol. 22, No. 3, 2008, pp. 399–406. doi:10.2514/1.33505

[19] Colonna, G., and Capitelli, M., "A Few Level Approach for the Electronic Partition Function of Atomic Systems," *Spectrochimica Acta. Part B, Atomic Spectroscopy*, Vol. 64, No. 9, 2009, pp. 863–873. doi:10.1016/j.sab.2009.07.002

[20] Laux, C. O., "Radiation and Nonequilibrium Collisional Radiative Models," *Physico-Chemical Models for High Enthalpy and Plasma Flows*, Vol. 1, von Kármán Institute for Fluid Dynamicsm Rhode-Saint-Genese, Belgium, July 2002, pp. 1–55.

[21] Colonna, G., Pietanza, L.-D., and Capitelli, M., "Coupled Solution of a Time-Dependent Collisional-Radiative Model and Boltzmann Equation for Atomic Hydrogen Plasmas: Possible Implications with LIBS Plasmas," *Spectrochimica Acta. Part B, Atomic Spectroscopy*, Vol. 56, No. 6, 2001, pp. 587–598. doi:10.1016/S0584-8547(01)00223-3

[22] Bourdon, A., and Vervisch, P., "Three Body Recombination Rates of Atomic Nitrogen in Low Pressure Plasma Flows," *Physical Review E (Statistical Physics, Plasmas, Fluids, and Related Interdisciplinary Topics)*, Vol. 54, No. 2, 1996, pp. 1888–1898. doi:10.1103/PhysRevE.54.1888

[23] Bourdon, A., Térésiak, Y., and Vervisch, "Ionization and Recombination Rates of Atomic Oxygen in High Temperature Air Plasma Flows," *Physical Review E (Statistical Physics, Plasmas, Fluids, and Related Interdisciplinary Topics)*, Vol. 57, No. 4, 1998, pp. 4684–4692. doi:10.1103/PhysRevE.57.4684

[24] Drawin, H., "Zur formelmassigen Darstellung des Ionisierungs-querschnitts fur den Atom-Atomstoss und uber die Ionen-Elektronen-Rekombination im Dichten Neutralgas," *Zeitschrift fur Physik D: Atoms, Molecules and Clusters*, 1968, pp. 404–417.

[25] Drawin, H., "Atomic Cross Sections for Inelastic Collisions," Rept. EUR-CEA-FC 236, 1963.

[26] Bacri, J., and Medani, A., "Electron Diatomic Molecule Weighted Total Cross Section Calculation: I, Principles for Calculation," *Physica C*, Vol. 101, No. 3, 1980, pp. 399–409. doi:10.1016/0378-4363(80)90037-6

[27] Teulet, P., Sarrette, J.-P., and Gomes, A.-M., "Calculation Of Electron Impact Inelastic Cross Sections And Rate Coefficients For Diatomic Molecules," *Journal of Quantitative Spectroscopy and Radiative Transfer*, Vol. 1, No. 5, 1999, pp. 549–569. doi:10.1016/S0022-4073(98)00129-0

[28] Bacri, J., and Medani, A., "Electron Diatomic Molecule Weighted Total Cross Section Calculation II. Application to the Nitrogen Molecule," *Physica C*, Vol. 101, No. 3, 1980, pp. 410–419. doi:10.1016/0378-4363(80)90038-8

[29] Bacri, J., and Medani, A., "Electron Diatomic Molecule Weighted Total Cross Section Calculation III. Main Inelastic Processes for N_2 and N_2^+," *Physica C*, Vol. 112, No. 1, 1982, pp. 101–118. doi:10.1016/0378-4363(82)90136-X

[30] Sarrette, J.-P., Gomes A. M., Bacri, J., Laux, C. O., and Kruger, C. H., "Collisional-Radiative Modelling of Quasi-Thermal Air Plasmas With Electronic Temperatures Between 2000 And 13,000 K," *Journal of Quantitative Spectroscopy and Radiative Transfer*, Vol. 53, No. 2, 1995, pp. 125–141.

[31] Lotz, W., "Electron-Impact Ionization Cross Sections and Ionization Rate Coefficients for Atoms and Ions from Hydrogen to Calcium," *Zeitschrift fur Physik D: Atoms, Molecules and Clusters*, Vol. 216, No. 3, 1968, pp. 241–247.

[32] Capitelli, M., Ferreira, C., Gordiets, B., and Osipov, A., *Plasma Kinetics in Atmospheric Gases*, Springer, Berlin, 2000, pp. 1–303.

[33] Kossyi, I., Kostinsky, A., Matveyev, A., and Silakov, V., "Kinetic Scheme of the Non-Equilibrium Discharge in Nitrogen-Oxygen Mixtures," *Plasma Sources Science and Technology* , Vol. 1, No. 3, 1992, pp. 207–220. doi:10.1088/0963-0252/1/3/011

[34] Chaban, G., Jaffe, R., Schwenke, D., and Huo, W., "Dissociation Cross Sections and Rate Coefficients for Nitrogen from Accurate Theoretical Calculations," AIAA Paper 2008-1209, Jan. 2008.

[35] Jaffe, R., Schwenke, D., Chaban, G., and Huo, W., "Vibrational and Rotational Excitation and Relaxation of Nitrogen from Accurate Theoretical Calculations," AIAA Paper 2008-1208, Jan. 2008.

[36] Esposito, F., Armenise, I., and Capitelli, M., "N-N_2 State to State Vibrational Relaxation and Dissociation Rates Based on Quasiclassical Calculations," *Chemical Physics*, Vol. 331, No. 1, 2006, pp. 1–8. doi:10.1016/j.chemphys.2006.09.035

[37] Macheret, S., Fridman, A. A., Adamovich, I. V., Rich, J. W., and Treanor, C. E., "Mechanisms of Nonequilibrium Dissociation of Diatomic Molecules," AIAA Paper 1994-1984, 1994.

[38] Adamovich, V. I., Macheret, S. O., Rich, W. J., and Treanor, C. E., "Vibrational Energy Transfer Rates Using a Forced Harmonic Oscillator Model," *Journal of Thermophysics and Heat Transfer*, Vol. 2, No. 1, 1998, pp. 57–65. doi:10.2514/2.6302

[39] Chernyi, G. G., and Losev, S. A., Macheret, S. O., and Potapkin, B. V., *Physical and Chemical Processes in Gas Dynamics: Physical and Chemical Kinetics and Thermodynamics of Gases and Plasmas*, AIAA, Reston, VA, 2004, pp. 1–311.

[40] Macheret, S. O., and Adamovich, I. V., "N-N_2 Semiclassical Modeling of State-Specific Dissociation Rates in Diatomic Gases," *Chemical Physics*, Vol. 34, No. 17, 2000, pp. 7351–7361.

[41] Marrone, P. V., and Treanor, C. E., "Chemical Relaxation with Preferential Dissociation from Excited Vibrational Levels," *Physics of Fluids*, Vol. 6, No. 9, Sept. 1963, pp. 1215–1221. doi:10.1063/1.1706888

[42] Hammerling, P., Teare, J. D., and Kivel, B., "Theory of Radiation from Luminous Shock Waves in Nitrogen," *Physics of Fluids*, Vol. 2, July 1959, pp. 422–426. doi:10.1063/1.1724413

[43] Park, C., Jaffe, R., and Partridge, H., "Chemical-Kinetic Parameters of Hyperbolic Earth Entry," *Journal of Thermophysics and Heat Transfer*, Vol. 15, No. 1, 2001, pp. 76–90. doi:10.2514/2.6582

[44] Cosby, P., "Electron-Impact Dissociation of Nitrogen," *Journal of Chemical Physics*, Vol. 98, No. 12, 1993, pp. 9544–9553. doi:10.1063/1.464385

[45] Cosby, P., "Electron-Impact Dissociation of Oxygen," *Journal of Chemical Physics*, Vol. 98, No. 12, 1993, pp. 9560–9569. doi:10.1063/1.464387

[46] Guberman, S., *Electron-Vibration Exchange Models in Nitrogen Flows*, Kluwer, Dordrecht, The Netherlands, 2003.

[47] Bultel, A., van Ootegem, B., Bourdon, A., and Vervisch, P., "Influence of Ar_2^+ in an Argon Collisional-Radiative Model," *Physical Review E (Statistical Physics, Plasmas, Fluids, and Related Interdisciplinary Topics)*, Vol. 65, No. 4, 2002, Paper 046406. doi:10.1103/PhysRevE.65.046406

[48] Surzhikov, S., Sharikov, I., Capitelli, M., and Colonna, G., "Kinetic Model of Nonequilibrium Radiation of Strong Air Shock Waves," AIAA Paper 2006-586, Jan. 2006.

[49] Bose, D., and Candler, G., "Thermal Rate constants of the $N_2 + O \rightarrow NO + O$ reaction using ab initio 3 a and 3 a Potential-Energy Surfaces," *Journal of Chemical Physics*, Vol. 104, No. 8, 1996, pp. 2825–2833. doi:10.1063/1.471106

[50] Bose, D., and Candler, G., "Thermal Rate Constants of the $O_2 + N \rightarrow NO + O$ Reaction Using Ab Initio 3a and 3a Potential-Energy Surfaces," *Journal of Chemical Physics*, Vol. 107, No. 16, 1997, pp. 6136–6145. doi:10.1063/1.475132

[51] Lamet, J. M., Babou, Y., Riviere, P., Perrin, M. Y., and Soufiani, A., "Radiative Transfer in Gases Under Thermal and Chemical Nonequilibrium Conditions: Application to Earth Atmospheric Re-Entry," *Journal of Quantitative Spectroscopy and Radiative Transfer*, Vol. 109, No. 2, 2008, pp. 235–244. doi:10.1016/j.jqsrt.2007.08.026

[52] Martin, W. C., Fuhr, J. R., Kelleher, D. R., Masgrove, A., Sugar, J., and Wiese, W. L., "NIST Atomic Spectra Database (Version 2.0)," 1999, http://www.nist.gov/pml/data/asd.cfm [retrieved 2009].

[53] Laux, C., and Kruger, C., "Arrays of Radiative Transition Probabilities for the N_2 First and Second Positive, NO Beta and Gamma, N_2^+ First Negative and O_2 Schumann–Runge Band Systems," *Journal of Quantitative Spectroscopy and Radiative Transfer*, Vol. 48, No. 1, 1992, pp. 9–24; also AIAA Paper 1998-2664, 1998. doi:10.1016/0022-4073(92)90003-M

[54] Vincenti, W., and Kruger, C., *Introduction to Physical Gas Dynamics*, Wiley, New York, 1965, pp. 1–538.

[55] Magin, T. E., Caillault, L., Bourdon, A., and Laux, C. O., "Nonequilibrium Radiative Heat Flux Modeling for the Huygens Entry Probe," *Journal of Geophysical Research: Planets*, Vol. 111, 2006, Paper E07S12. doi:10.1029/2005JE002616

[56] Grinstead, J., Wilder, M., Olejniczak, J., Bogdanoff, D., Allen, G., Dang, K., and Forrest, M., "Shock-Heated Air Radiation Measurements at Lunar Return Conditions," AIAA Aerospace Sciences Meeting and Exhibit, Reno, NV, AIAA Paper 2008-1244, Jan. 2008.

[57] Panesi, M., Babou, Y., and Chazot, O., "Predictions of Nonequilibrium Radiation: Analysis and Comparison with East Experiments," 40th Thermophysics Conference, Seattle, WA, AIAA Paper 2008-3812, June 2008.

[58] Gorelov, V., Kildushova, L., and Kireev, A., "Ionization Particularities Behind Intensive Shock Waves in Air at Velocities of 8–15 km/s," AIAA Paper 1994-2051, June 1994.

[59] Zeldovich, Y., and Raizer, Y., *Physics of Shock Waves and High Temperature Hydrodynamic Phenomena*, Academic Press, London, 1966, pp. 1–464.

[60] Mitchner, M., and Kruger, C., *Partially Ionized Gases*, Wiley, New York, 1973, pp. 1–497.

[61] Park, C., "Radiation Enhancement by Nonequilibrium in Earth's Atmosphere," *Journal of Spacecraft and Rockets*, Vol. 22, No. 1, 1985, pp. 27–36.
doi:10.2514/3.25706

[62] Kunc, J. A., and Soon, W. H., "Collisional-Radiative Non-Equilibrium in Partially-Ionized Atomic Nitrogen," *Physical Review A*, Vol. 40, No. 10, 1989, pp. 5822–5843.
doi:10.1103/PhysRevA.40.5822

[63] Kunc, J. A., and Soon, W. H., "Thermal Nonequilibrium in Partially Ionized Atomic Oxygen," *Physical Review A*, Vol. 41, No. 2, 1990, pp. 825–843.
doi:10.1103/PhysRevA.41.825

[64] Cambier, J. L., and Moreau, S., "Simulations of a Molecular Plasma in Collisional-Radiative Nonequilibrium," AIAA 24th Plasmadynamics and Lasers Conference, Orlando, FL, AIAA Paper 1993-3196, July 1993.